Journal of Sound and Vibration (2000) **233**(2), 235–254
doi:10.1006/jsvi.1999.2811, available online at http://www.idealibrary.com on IDEAL®

ROCK DESTRUCTION EFFECT ON THE STABILITY OF A DRILLING STRUCTURE

N. CHALLAMEL

Ecole Nationale Supérieure des Mines de Paris, Centre de Géotechnique et d'Exploitation du Sous-sol, 35 rue Saint-Honoré, 77305 Fontainebleau, France

(*Received* 21 *June* 1999, *and in final form* 15 *October* 1999)

The motion of a drilling structure is studied in torsion. The stability of the stationary solution is determined by the direct method of Liapounov, supplemented with results for the linearized method. The stability criterion is firmly based on the form of the boundary condition linked to the rock destruction process. This rock/bit interaction function can be deduced using studies on rock mechanics, based on yield design formalism. Assuming a quasi-static axial evolution, numerical simulations illustrate the instability of the stationary solution: the bit motion can converge on a limit cycle, often called stick–slip. The beam therefore evolves as a complex cone-shaped limit surface. A simple two-degrees-of-freedom system is now considered in both axial and torsional directions, to quantify the quasi-static axial assumption. The instability of the stationary solution is confirmed by the linearized method for the undamped system with the postulated boundary conditions. Even for small damping values the same result is achieved. Even though a limit cycle appears in the axial plane (small amplitude), stick–slip can be described adequately by considering a quasi-static axial evolution.

1. INTRODUCTION

Drill string vibrations are generally quite complex. Axial, lateral and torsional vibrations are present and sometimes coupled. Phenomena such as bit bouncing, whirling or stick–slip have all been shown to occur. A full simulation covering all relevant phenomena is not reasonably practical and authors generally study vibration mechanisms individually. The main difficulty is modelling the boundary conditions especially the rock/bit interaction which cannot be determined precisely in complex bit kinematics (for instance in the case of lateral vibrations). Torsional drill string vibrations, also known as stick–slip, contribute to drillpipe fatigue and are detrimental to bit life. They can also affect the rate of penetration (ROP) and the instantaneous efficiency of the installation, and occur for more than 50% of the total time of a classical rig step [1]. The purpose of this paper is to consider this parasitic non-linear phenomenon, using knowledge of rock mechanics for identification of the boundary condition. The study is limited to polycrystalline diamond compact (PDC) bits although some analogies to roller bits could be pertinent.

Authors often favour a detailed description of the drill string and restrict the boundary condition to a harmonic [2] or a constant [3] loading. It is shown in this paper that the rock/bit interaction, linked to the rock destruction process, is a non-linear function, which conducts to an autonomous dynamic system. With the type of boundary conditions postulated, Belyaev and Brommundt [4] proposed a stability study for a linearized system with a surface motor, resulting in only the necessary instability conditions. Dunayevsky

0022-460X/00/220235 + 20 $35.00/0

and Abbassian [5] gave stability conditions for a linearized one-degree-of-freedom system. The present study defines the stability conditions for the stationary solution of the real continuous medium, using the direct method of Liapounov. The linearized motion is also considered to complement the stability investigation. Finally, the induced non-linear phenomenon is illustrated by numerical simulations.

2. STATEMENT OF THE PROBLEM

The drillpipe is considered as a beam in torsion. A lumped inertia I_B is chosen to represent the bottomhole assembly. A damping β, which includes the viscous and structural damping, is assumed along the structure. The speed at the surface ($x = 0$) is restricted to a constant value Ω, and the other extremity ($x = L$), which symbolizes the bit, is subjected to a torque φ, which is a function of the bit speed (this point will be justified later). The mechanical system is described by the following equations [6]:

$$\begin{gathered} GJ\frac{\partial^2 u}{\partial x^2}(x,t) - I\frac{\partial^2 u}{\partial t^2}(x,t) - \beta\frac{\partial u}{\partial t}(x,t) = 0, \quad x \in D = [0;L], \quad \beta \geqslant 0, \\ u(0,t) = \Omega t, \qquad GJ\frac{\partial u}{\partial x}(L,t) + I_B\frac{\partial^2 u}{\partial t^2}(L,t) = -\varphi\left(\frac{\partial u}{\partial t}(L,t)\right), \end{gathered} \tag{1}$$

where $u(x,t)$ is the angle of rotation, I is the inertia, G is the shear modulus, J the geometrical moment of inertia.

The existence and uniqueness of the solution are assumed to be obtained for all the initial conditions. The stationary solution $u^0(x,t)$ of this system is

$$u^0(x,t) = \Omega t - \left(\frac{\varphi(\Omega)}{GJ} + \frac{\beta\Omega}{GJ}L\right)x + \frac{\beta\Omega}{2GJ}x^2. \tag{2}$$

The change of variable $v(x,t) = u(x,t) - u^0(x,t)$ leads to an equivalent autonomous system, for which the function $v^0(x,t) \equiv 0$ is a solution:

$$\begin{gathered} GJ\frac{\partial^2 v}{\partial x^2}(x,t) - I\frac{\partial^2 v}{\partial t^2}(x,t) - \beta\frac{\partial v}{\partial t}(x,t) = 0, \quad x \in D = [0;L], \\ v(0,t) = 0, \qquad GJ\frac{\partial v}{\partial x}(L,t) + I_B\frac{\partial^2 v}{\partial t^2}(L,t) = \varphi(\Omega) - \varphi\left(\Omega + \frac{\partial v}{\partial t}(L,t)\right). \end{gathered} \tag{3}$$

The end $x = 0$ is now fixed and the wave propagation equation has not changed. The stability of the trivial solution $v^0(x,t)$ of equation (3) is equivalent to the stability of $u^0(x,t)$ of equation (1).

3. STABILITY ANALYSIS OF THE CONTINUOUS MEDIUM

3.1. DIRECT METHOD OF LIAPOUNOV

The Hilbert space $H_0^1(D) \times L^2(D)$, which includes the inner product associated with the norm energy H, is introduced:

$$H = \int_0^L \frac{1}{2}GJ\left(\frac{\partial v}{\partial x}(x,t)\right)^2 \mathrm{d}x + \int_0^L \frac{1}{2}I\left(\frac{\partial v}{\partial t}(x,t)\right)^2 \mathrm{d}x + \frac{1}{2}I_B\left(\frac{\partial v}{\partial t}(L,t)\right)^2. \tag{4}$$

Differentiating with respect to t that follows from equation (4)

$$\dot{H} = \int_0^L GJ \frac{\partial v}{\partial x}(x,t) \frac{\partial^2 v}{\partial x \partial t}(x,t)\,\mathrm{d}x + \int_0^L I \frac{\partial v}{\partial t}(x,t) \frac{\partial^2 v}{\partial t^2}(x,t)\,\mathrm{d}x + I_B \frac{\partial v}{\partial t}(L,t) \frac{\partial^2 v}{\partial t^2}(L,t). \quad (5)$$

An integration by parts of the first term leads to

$$\dot{H} = GJ \left[\frac{\partial v}{\partial x}(x,t) \frac{\partial v}{\partial t}(x,t) \right]_0^L + \int_0^L \frac{\partial v}{\partial t}(x,t) \left[I \frac{\partial^2 v}{\partial t^2}(x,t) - GJ \frac{\partial^2 v}{\partial x^2}(x,t) \right] \mathrm{d}x + I_B \frac{\partial v}{\partial t}(L,t) \frac{\partial^2 v}{\partial t^2}(L,t). \quad (6)$$

The introduction of boundary conditions and wave equation gives

$$\dot{H} = \frac{\partial v}{\partial t}(L,t) \left[\varphi(\Omega) - \varphi\left(\Omega + \frac{\partial v}{\partial t}(L,t) \right) \right] - \int_0^L \beta \left(\frac{\partial v}{\partial t}(x,t) \right)^2 \mathrm{d}x. \quad (7)$$

$$\text{Hence, } \varphi \text{ monotonously increasing} \Rightarrow \frac{\mathrm{d}H}{\mathrm{d}t} \leqslant 0. \quad (8)$$

H is a Liapounov functional by conception. The application of Liapounov's theorem (extended by Movchan [7, 8] for continuous media) results in:

$$\varphi \text{ monotonously increasing} \Rightarrow \left(v(x,t), \frac{\partial v}{\partial t}(x,t) \right) = (0,0) \text{ stable}. \quad (9)$$

The stability is naturally relative to the metric used; that is, to the total energy norm. When φ is decreasing, a general conclusion is not possible. The damping and decrease of φ have the opposite effect in term of stability (see equation (7)).

For the undamped system ($\beta = 0$), only the rock–bit interaction function φ governs the stability of the stationary solution. If φ is strictly increasing, the stationary solution is asymptotically stable. This result can be shown, using the Lassale invariance principle [9, 10]. Trajectories of the system tend to the largest invariance set contained in the subspace of constant energy ($\dot{H} = 0$). This subspace is determined by an "over conditional" system which allows only one solution $v^0(x,t)$. The stability condition follows:

$$\varphi \text{ monotonously strictly increasing} \Rightarrow (0,0) \text{ is asymptotically stable}. \quad (10)$$

The attraction basin is then the sole functional space. From a more general point of view, it is sufficient that φ is increasing and is bijective around Ω to ensure the stability. If φ is a constant function, the problem is reduced to the particular case of a fixed beam with a free end, for which the trivial solution is stable. Finally, if φ is decreasing, the eigenvalues of the linearized system can be calculated explicitly when I_B vanishes, and all have a positive real part. Although the eigenvalue problem cannot be analytically solved in the general case, the previous result let us think that the stationary solution is still unstable for all values of I_B.

3.2. LINEARIZED SYSTEM

Considering the linearized undamped system without lumped inertia ($\beta = I_B = 0$),

$$I\frac{\partial^2 v}{\partial t^2}(x,t) = GJ\frac{\partial^2 v}{\partial x^2}(x,t),$$
$$v(0,t) = 0, \qquad GJ\frac{\partial v}{\partial x}(L,t) = -\varphi'(\Omega)\frac{\partial v}{\partial t}(L,t). \tag{11}$$

The solution is sought in the form $v(x,t) = \psi(x)\mathrm{e}^{\lambda t}$.

Using the wave equation, $v(x,t)$ can be written as

$$v(x,t) = C_1\mathrm{e}^{\lambda(t+x/c)} + C_2\mathrm{e}^{\lambda(t-x/c)}$$

with $c = \sqrt{GJ/I}$, torsional wave celerity and $\lambda \in \mathbb{C}$.

The boundary conditions lead to the characteristic system

$$C_1 + C_2 = 0,$$
$$\lambda\sqrt{IGJ}\,(C_1\mathrm{e}^{\lambda\sqrt{I/GJ}\,L} + C_2\mathrm{e}^{-\lambda\sqrt{I/GJ}\,L}) = -\varphi'(\Omega)\lambda\,(C_1\mathrm{e}^{\lambda\sqrt{I/GJ}\,L} + C_2\mathrm{e}^{-\lambda\sqrt{I/GJ}\,L}). \tag{12}$$

This system allows a non-trivial solution if

$$\mathrm{e}^{2\lambda\sqrt{I/GJ}L} = \frac{\varphi'(\Omega) - \sqrt{IGJ}}{\varphi'(\Omega) + \sqrt{IGJ}}. \tag{13}$$

Now set $\lambda = a + \mathrm{i}b$, where $(a,b) \in \mathbb{R}^2$.

The following equality must be satisfied:

$$\mathrm{e}^{2a\sqrt{I/GJ}L} = \eta\frac{\varphi'(\Omega) - \sqrt{IGJ}}{\varphi'(\Omega) + \sqrt{IGJ}} \quad \text{with } \eta = \pm 1.$$

Four cases can be drawn:

- $\varphi'(\Omega) \in \left]\sqrt{IGJ}; +\infty\right] \Rightarrow \eta = +1\left(b = k\frac{\pi}{L}\sqrt{\frac{GJ}{I}}\right) \Rightarrow a < 0.$
- $\varphi'(\Omega) \in \left]0; \sqrt{IGJ}\right[\Rightarrow \eta = -1\left(b = \left(\frac{2k+1)\pi}{2L}\right)\sqrt{\frac{GJ}{I}}\right) \Rightarrow a < 0.$
- $\varphi'(\Omega) \in \left]-\sqrt{IGJ}; 0\right[\Rightarrow \eta = -1\left(b = \frac{(2k+1)\pi}{2L}\sqrt{\frac{GJ}{I}}\right) \Rightarrow a > 0.$
- $\varphi'(\Omega) \in \left]-\infty; -\sqrt{IGJ}\right[\Rightarrow \eta = +1\left(b = k\frac{\pi}{L}\sqrt{\frac{GJ}{I}}\right) \Rightarrow a > 0.$

As a singular property, the real spectral distribution is invariant with the imaginary part. For the well-known case $\varphi'(\Omega) = 0$, a vanishes and the natural pulsations are $(2k+1)(\pi/2L)\sqrt{GJ/I}$. The sign of $\varphi'(\Omega)$ governs the sign of a. When φ is increasing, the real part of eigenvalues is negative (the result of stability is again found, but only for small perturbations). When φ is decreasing, the real part of eigenvalues is positive and the stationary solution is unstable. The motion can be expressed by

$$v(x,t) = \mathrm{e}^{at}\,\mathrm{Re}\left[\sum_{k\in\mathbb{N}} C_k \mathrm{e}^{\mathrm{i}b_k t}\left(\mathrm{e}^{ax/c}\,\mathrm{e}^{\mathrm{i}b_k x/c} - \mathrm{e}^{-ax/c}\mathrm{e}^{-\mathrm{i}b_k x/c}\right)\right] \quad \text{where } C_k = \alpha_k + \mathrm{i}\beta_k. \tag{14}$$

The series converge on the solution studied for the following generalized coordinate C_k. The following initial conditions can be introduced:

$$v(x,0) = \sum_{k\in\mathbb{N}}\left[\left(\mathrm{e}^{ax/c} - \mathrm{e}^{-ax/c}\right)\alpha_k \cos\left(b_k\frac{x}{c}\right) - \left(\mathrm{e}^{ax/c} + \mathrm{e}^{-ax/c}\right)\beta_k \sin\left(b_k\frac{x}{c}\right)\right]$$

$$\dot{v}(x,0) = av(x,0) + \sum_{k\in\mathbb{N}}\left[-\left(\mathrm{e}^{ax/c} + \mathrm{e}^{-ax/c}\right)\alpha_k b_k \sin\left(b_k\frac{x}{c}\right) - \left(\mathrm{e}^{ax/c} - \mathrm{e}^{-ax/c}\right)\beta_k b_k \cos\left(b_k\frac{x}{c}\right)\right]. \tag{15}$$

For $a = 0$, this system is reduced to

$$v(x,0) = -2\sum_{k\in\mathbb{N}} \beta_k \sin\left(b_k\frac{x}{c}\right),$$

$$\dot{v}(x,0) = -2\sum_{k\in\mathbb{N}} \alpha_k b_k \sin\left(b_k\frac{x}{c}\right). \tag{16}$$

The system of eigenfunctions $\sin(b_k x/c)$ is known to be complete. α_k and β_k can be written as

$$\beta_k = -\frac{1}{L}\int_0^L v(x,0)\sin\left(b_k\frac{x}{c}\right)\mathrm{d}x,$$

$$\alpha_k b_k = -\frac{1}{L}\int_0^L \dot{v}(x,0)\sin\left(b_k\frac{x}{c}\right)\mathrm{d}x. \tag{17}$$

The general solution of the complex system (15) can easily be proposed when an additional condition ($\alpha_k = 0$ for instance) is imposed. In the same way, it follows that

$$\beta_k = \frac{2}{L}\int_0^L \frac{-v(x,0)}{\left(\mathrm{e}^{ax/c} + \mathrm{e}^{-ax/c}\right)}\sin\left(b_k\frac{x}{c}\right)\mathrm{d}x. \tag{18}$$

The initial rotation speed condition leads to the constraint

$$\dot{v}(x,0) = v(x,0)\left[a - \left(\frac{\mathrm{e}^{ax/c} - \mathrm{e}^{-ax/c}}{\mathrm{e}^{ax/c} + \mathrm{e}^{-ax/c}}\right)^2\right] + v'(x,0)\left(\frac{\mathrm{e}^{ax/c} - \mathrm{e}^{-ax/c}}{\mathrm{e}^{ax/c} + \mathrm{e}^{-ax/c}}\right). \tag{19}$$

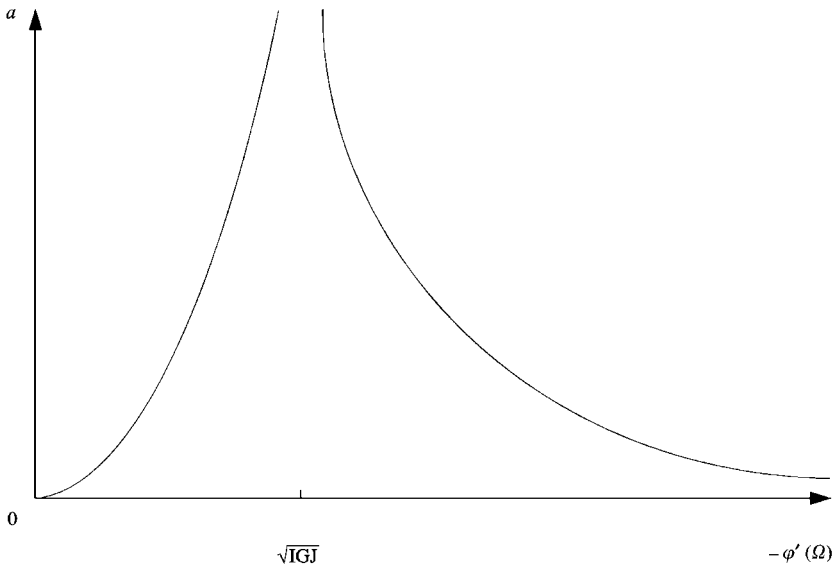

Figure 1. Sensitivity of the a parameter to φ.

Numerical calculation should be used for the more general case. Using the convergence property of $v(x + ct, 0)$ and $v(x - ct, 0)$, the convergence of $v(x, t)$ is immediately obtained. As a consequence, it follows that

$$\lim_{t \to \infty} \left(\frac{\ln \| v(x,t) \|}{t} \right) = a. \tag{20}$$

Here a symbolizes the evolution order of the perturbed motion. Figure 1 shows a graphical representation of a, defined in equation (20), versus $\varphi'(\Omega)$. The function a is an impair function, defining it on the whole plane. A singularity appears when $|\varphi'(\Omega)| = \sqrt{IGJ}$. This phenomenon, which should be attenuated by damping, can be likened to an autonomous resonance. Nevertheless, $|\varphi'(\Omega)|$ is generally small in drilling and only the first part of the graph is of significance.

When I_B cannot be neglected, the eigenvalues cannot be explicitly calculated. It is necessary to solve a transcendental complex equation. The direct method of Liapounov is then especially useful in this more realistic case.

4. ROCK/BIT INTERACTION FUNCTION

In stick–slip conditions, for sufficiently slow conditions (the stick–slip frequency is lower than the fundamental natural frequency as will be seen later), the interaction function can be described with the mean values of the instantaneous parameters during one revolution.

To quantify this function, the rock deformability is now considered. The drilling tool is composed of many elementary cutters, symbolized by rigid wedges. The rock reaction is quantified, using yield design formalism, which surrounds the maximum force potentially

bearable by the rock structure in a given kinematics [11]. The analysis is conducted in quasi-static outline in plane deformations. Tests performed in the laboratory show the independence of maximal forces with regard to speed over a range representative of drilling speeds. The maximal forces are theoretically proportional to the cutting area, although experimental limits of such a consideration have been shown [12, 13]. The proportionality coefficient, shown as ε, is called the specific energy. ε is a function of the Coulomb criterion and signifies the rock cutting hardness, for a given kinematics. The mean force is deduced by an empirical factor and the chipping cycle induced at this level is neglected. The integration of these local forces gives the global interaction function.

Now consider the axial bit position X and the torsional angle Y. $u(L,t)$, introduced earlier is denoted as Y here for the purpose of simplification. Assuming a sufficiently slow evolution of parameters $(\dot{X}, \dot{Y})$ during a period of bit revolution, the global interaction function can be approximated by a simple autonomous form. It is necessary for the number of bit revolutions during a stick–slip phase (ratio between Ω and the fundamental pulsation) to be sufficient to ensure the validity of this analytical expression. This assumption becomes pertinent when the ratio is greater than two; certain bit symmetrical considerations weaken the assumption.

The torque on the bit φ, resulting from the integration of local torques on the bit profile of R radius [14], is expressed by the bi-variable function

$$\varphi(\dot{X}, \dot{Y}) = z(\dot{X}, \dot{Y})\varepsilon \frac{R^2}{2}. \tag{21}$$

The coupling law z (depth of cut per revolution) governs the qualitative response of the system. This function is defined by

$$z(\dot{X}, \dot{Y}) = 2\pi \frac{\dot{X}}{\dot{Y}}. \tag{22}$$

In an equivalent way, the torque can be obtained by

$$\varphi(\dot{X}, \dot{Y}) = \pi\varepsilon R^2 \frac{\dot{X}}{\dot{Y}}. \tag{23}$$

The kinematic change for very slow rotation speed nevertheless defines a mode of indentation of rock (different from the classical functioning cutting mode), resulting in a finite torque when the rotation speed tends to zero (the bit axial speed is always positive for this bit type [15]). The hyperbolic function (23) is then corrected by an exponential decreasing law. The inverse functioning of the bit for negative rotation speed is taken into account. The interaction function can be written as

$$\begin{aligned} \varphi(\dot{X}, \dot{Y}) &= \zeta \dot{X} \mathrm{e}^{-\alpha \dot{Y}} \quad \text{if } \dot{Y} \geqslant 0, \\ \varphi(\dot{X}, \dot{Y}) &= -\zeta \dot{X} \quad \text{if } \dot{Y} < 0. \end{aligned} \tag{24}$$

ζ denotes the ability of the rock to be cut (a function of ε and R). The weight on bit (WOB) is approached analytically, using the same reasoning which led to the torque determination. The resulting linear relation between the torque and the bit is given by

$$\mathrm{WOB}(\dot{X}, \dot{Y}) = \mu\varphi(\dot{X}, \dot{Y}). \tag{25}$$

μ depends on the bit geometry (bit radius, rake angle) and is easily obtained for a flat bit [14].

5. STICK–SLIP SIMULATION

5.1. BIT MOTION

As a first step, the axial evolution is assumed to be quasi-static, or more precisely, the weak variation of $\dot{X}$ around its mean value is assumed to have no major influence on the torsion evolution, assuming that

$$\dot{X} = \mathrm{ROP}. \tag{26}$$

A coupled numerical study will confirm this hypothesis. Moreover, it does not contradict the small values of axial acceleration measured on rig for this bit [15].
The univariable φ function (linked with the Section 3) is now restricted to

$$\begin{aligned} &\varphi(\mathrm{ROP}, \dot{Y}) = \varphi^0 \mathrm{e}^{-\alpha \dot{Y}} \quad \text{if } \dot{Y} \geqslant 0 \\ &\varphi(\mathrm{ROP}, \dot{Y}) = -\varphi^0 \quad \text{if } \dot{Y} < 0 \end{aligned} \qquad \text{with } \varphi^0 = \zeta \mathrm{ROP}. \tag{27}$$

This convex decreasing form is observed during drilling (see references [15–17] for instance). It can generate the instability of the stationary motion.

Numerical simulations illustrate the induced phenomenon with the finite difference method (simulation of equation (1)). Twenty elements mesh the structure and the equation of motion is solved with the fourth order Runge–Kutta algorithm. The initial speed is equal to Ω and the initial rotation is chosen to be equal to zero for all points, thus affecting the stationary solution. The drillstring is a pipe made of steel (density ρ, Young's modulus

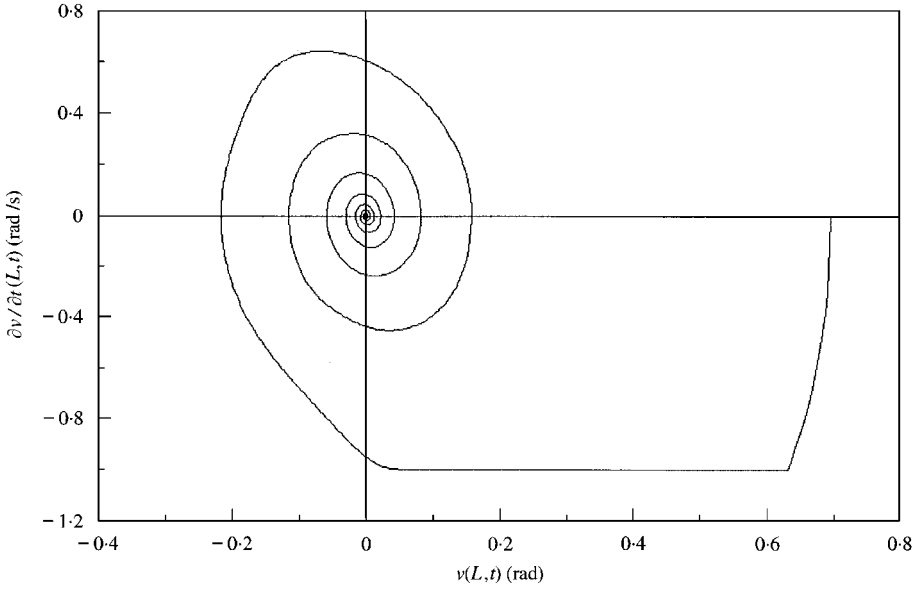

Figure 2. Asymptotical stability—$\beta = 0{\cdot}5$ N s.

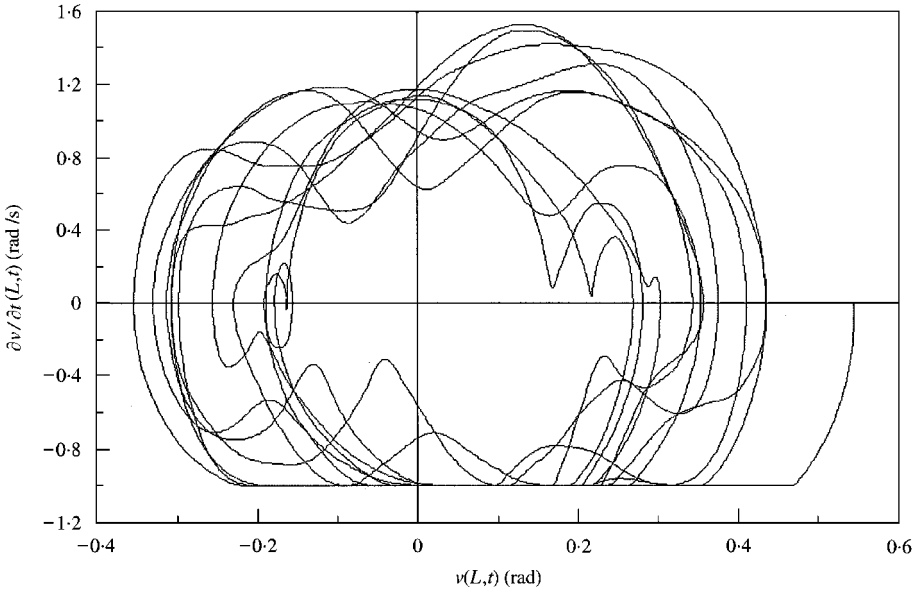

Figure 3. Stick–slip simulation—undamped system.

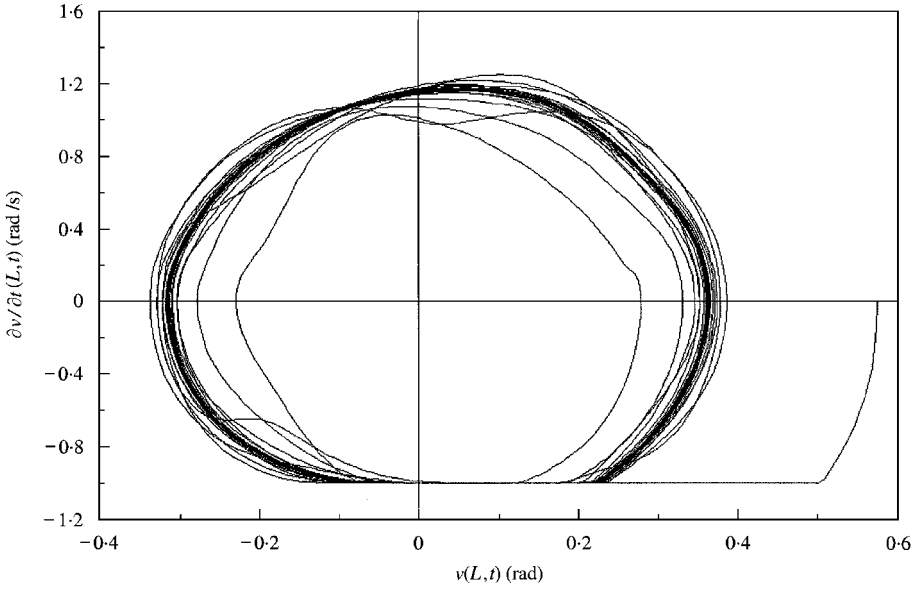

Figure 4. Stick–slip simulation—$\beta = 0{\cdot}1$ N s.

E and the Poisson ratio v). Its geometry is defined by its external diameter D_{ext} and internal diameter D_{int}. The representative values, chosen for the simulation, are

$L = 1000\,\text{m}$, $\rho = 8000\,\text{Kg/m}^3$, $E = 2 \times 10^5\,\text{MPa}$, $v = 0{\cdot}3$, $D_{ext} = 0{\cdot}127\,\text{m}$, $D_{int} = 0{\cdot}079\,\text{m}$,

$I_B = 89\ \text{Kg m}^2$, $\Omega = 1\ \text{rad/s}$, $\varphi^0 = 1000\,\text{N m}$, $\alpha = 0{\cdot}1\,\text{s}$.

Figures 2–4 represent the trajectory in the bit space phase with the relative variable v, for different damping values. The initial bit speed is zero in this plane, which corresponds to the extremity of the trajectory on the right-hand side of the figures. The stick phase was numerically treated by fixing the bit speed (this procedure is detailed in next section). The trajectory follows a global rotation motion clockwise. For a large damping value, the motion is asymptotically stable and trajectories converge on the stationary solution (Figure 2).

A structural perturbation (an increase of α, which grows with the rock hardness or a decrease of β) can generate a bifurcation of the system [17]. At least one of the real parts of the eigenvalues crosses the imaginary axis and the motion converges on stick–slip (Figures 3 and 4).

The minimal speed is zero (absolute variable u) and the maximal speed is greater than twice Ω. For the undamped system (Figure 3), trajectories are ruled by initial conditions and do not converge on the limit cycle (the attractor seems to be almost-periodical). The motion is simulated over 20 s, in this case corresponding to a few cycles. The attractor changes with some damping (Figure 4) and becomes a limit cycle. The stick–slip period is less than the natural fundamental frequency (0·52 Hz in the example instead of 0·53 Hz).

5.2. BEAM MOTION

In this final case ($\beta = 0{\cdot}1$ N s), the extremity of the beam describes a limit cycle well known in other dynamical systems. In reality, the beam converges on a cone-shaped limit surface. A three-dimensional view is shown in Figure 5. This surface is projected on a plane perpendicular to the beam neutral axis (stationary solution), for the different discretization

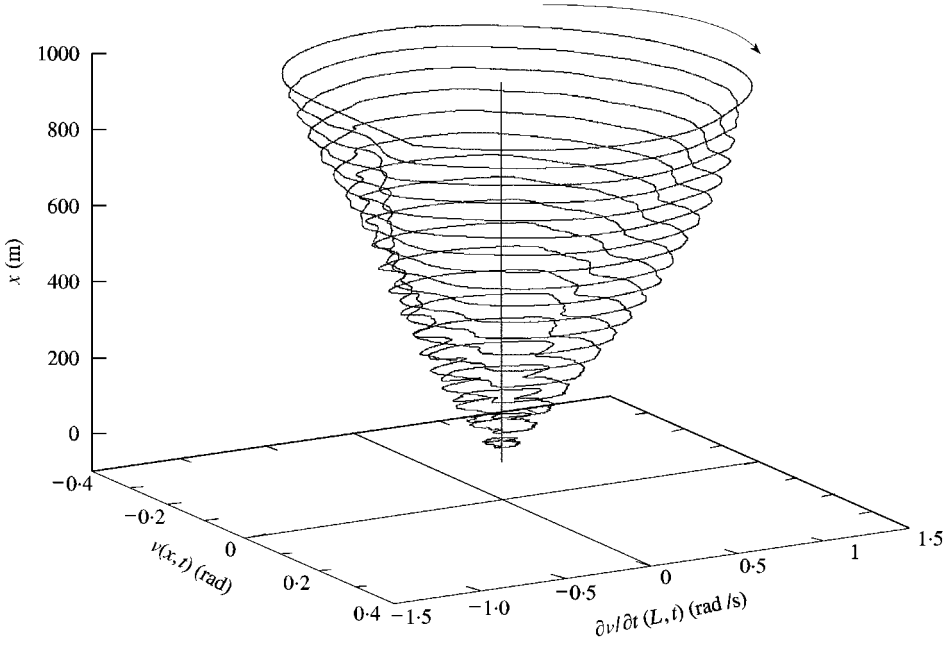

Figure 5. Three-dimensional view of the limit surface.

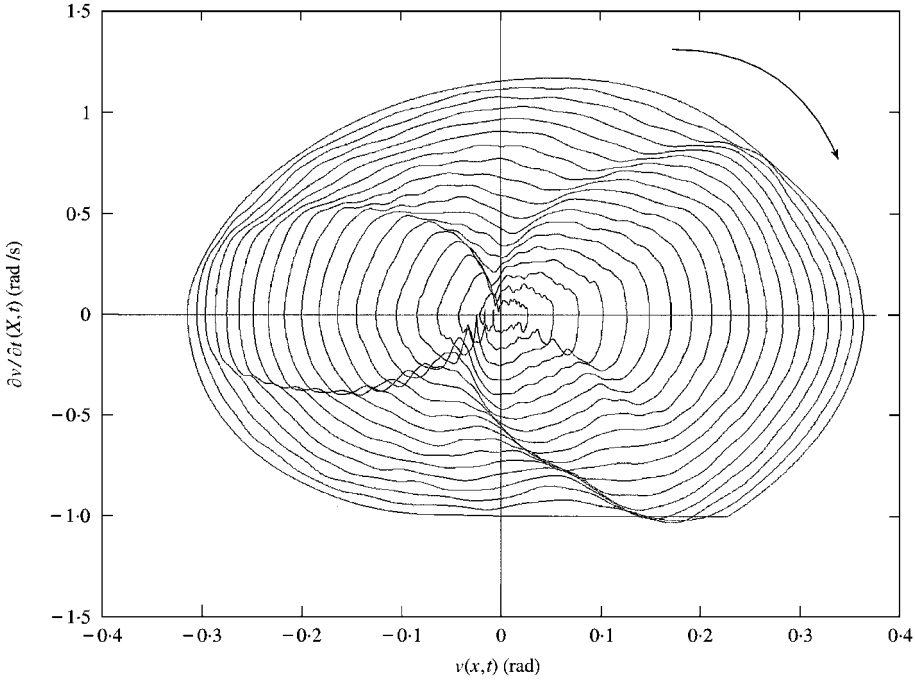

Figure 6. Projected limit surface.

points (Figure 6). The bit limit can be recognized with the typical stick phase in Figure 6. The propagation of the sudden bit stick phase can also be seen. In particular, some beam points above the bit reach negative speed (in terms of u variable). The amplitude of limit cycles tends to decrease while going up to the surface, until the limit cycle becomes a point at the surface. The complex form of each of these cycles (and in a global way of the limit surface) depends on the structural parameter chosen.

The beam motion has been photographed each 0·1 s, to cover the limit surface with about 20 pictures. Figure 7 represents the beam rotation and Figure 8 the beam rotation speed.

The arrows indicate the direction of evolution of the beam. As the limit surface does not display any axial symmetry, it has been necessary to represent the beam motion in both directions. This asymmetry is especially marked for the beam rotation speed. During the stick phase, the bit rotation speed is fixed, generating a spectacular wave in the beam. It can also be noticed that rotation is not linear along the beam, as opposed to the static solution.

6. COUPLED MOTION STUDY

The drilling structure is modelled in the torsional and axial directions to verify the previous assumption. Any static or dynamical buckling phenomenon is ignored (even if BHA presence decreases such a risk) and an axial hypothesis is quantified by this new dynamical model. This subject is rarely considered in the literature. This type of coupling

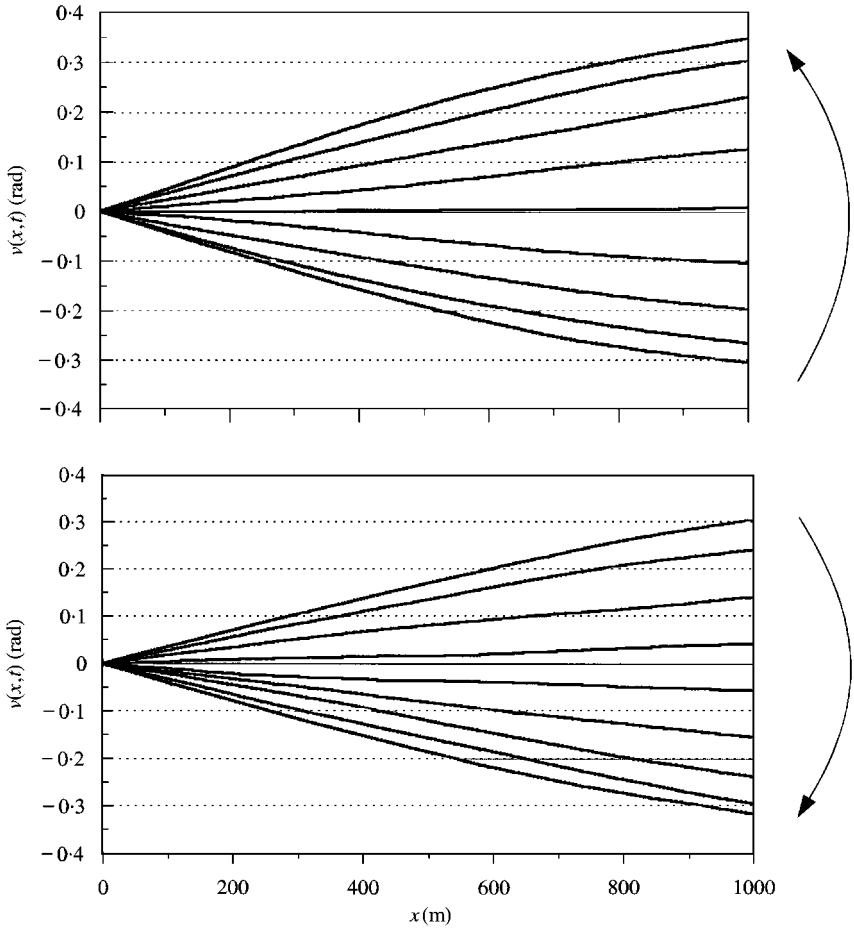

Figure 7. Evolution of the beam rotation of each 0·1 s during one cycle.

was studied with a harmonic loading [18] applied to roller cone bits. A mesh of the bottomhole profile, to calculate the cutting areas at any time, did not succeed in determining any clear tendency [19]. Moreover, this total numerical study exhibits the constancy of the bit axial speed during a large range of stick–slip. The third part has shown in only a torsional study the major role of the rock/bit interaction in the drilling structure dynamics.

6.1. REDUCTION TO A ONE-DEGREE-OF-FREEDOM SYSTEM

The drillpipe is initially only considered in torsion. A simplified one-degree-of-freedom model is proposed to evaluate the pertinence of such a simplification. The stick–slip frequency is only a little lower than the fundamental natural frequency of the continuous system. The reduction is studied for the linearized system at the first mode and the non-linear correspondence will be justified with a numerical comparison. The Ritz method [20, 21] gives the approximation of the characteristics of the first mode. It is much better the rotation of the first mode becomes linear (I_B great before $I \times L$).

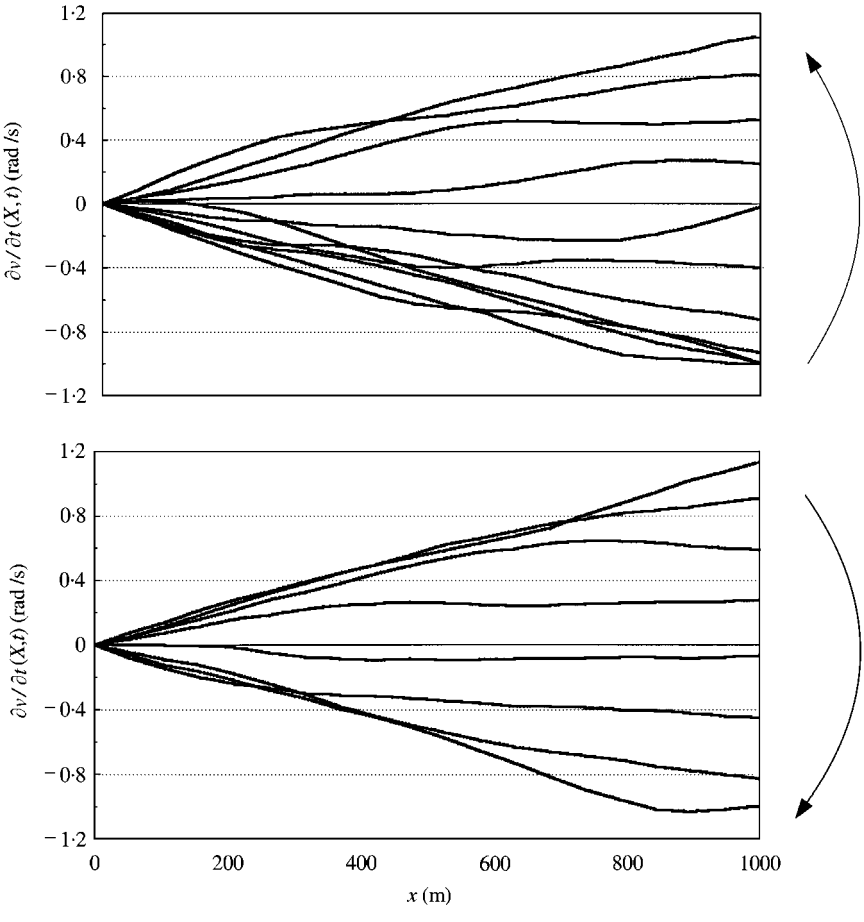

Figure 8. Evolution of the beam rotation of each 0·1 s during one cycle.

A linear interpolation of the field displacement along the beam is assumed. This gives

$$m_1 = I_B + \int_0^L I\left(\frac{x}{L}\right)^2 \mathrm{d}x = I_B + \frac{IL}{3},$$

$$c_1 = \beta\int_0^L \left(\frac{x}{L}\right)^2 \mathrm{d}x = \frac{\beta L}{3}, \tag{28}$$

$$k_1 = GJ\int_0^L \left(\frac{1}{L}\right)^2 \mathrm{d}x = \frac{GJ}{L},$$

where m_1 is the mass, k_1 the stiffness and c_1 the modal damping.

The motion is expressed by

$$m_1\ddot{Y} + c_1\dot{Y} + k_1(Y - \Omega t) = -\varphi(\mathrm{ROP}, \dot{Y}). \tag{29}$$

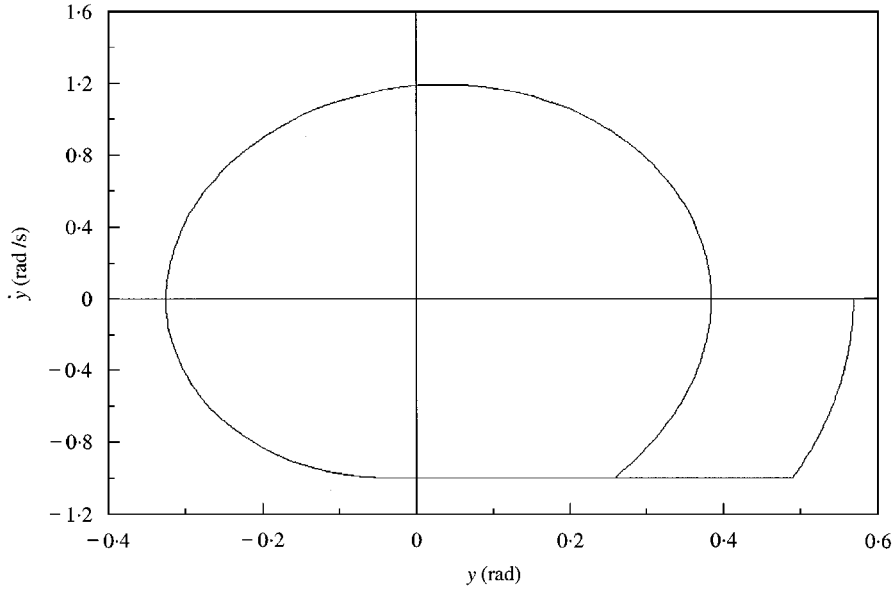

Figure 9. Stick–slip—uncoupled case of the one-degree-of-freedom system.

The change of variable adopted is

$$y = Y - \Omega t + \frac{\varphi(\mathrm{ROP}, \Omega)}{k_1} + \frac{c_1 \Omega}{k_1}. \tag{30}$$

The new system, which admits the trivial solution, can be expressed by

$$m_1 \ddot{y} + c_1 \dot{y} + k_1 y = \varphi(\mathrm{ROP}, \Omega) - \varphi(\mathrm{ROP}, \Omega + \dot{y}). \tag{31}$$

The following initial conditions have been chosen to link this part with the previous one: $y_0 = 0{\cdot}57$ rad. The initial speed $\dot{y}_0$ is equal to zero (similar to the parameters given in Section 5). The fourth order Runge–Kutta algorithm has been used to solve the non-linear problem and the classical numerical treatment of the stick phase has been proposed to describe this specific phenomenon. During the stick phase, an additional condition is given by the value of the speed equal to $-\Omega$. The torque is liberated and then equal to

$$\varphi(\mathrm{ROP}, 0) = \varphi(\mathrm{ROP}, \Omega) + c\Omega - ky. \tag{32}$$

A comparison of the motion of the continuous system with the motion of the associated one-degree-of-freedom system is then proposed. The classical stick–slip phenomenon can be seen in Figure 9. A discontinuity in the slope appears when the bit begins to stick, in contrast to the end of the stick phase. The limit cycle simulated is very similar to the limit cycle obtained with the total beam discretization (Figure 4). Only the transitory phase is significantly different. A frequential comparison quantifies the validity of the simplified approach. The Ritz method slightly overestimates the fundamental natural frequency of the real system (0·54 Hz instead of 0·53 Hz). The limit cycle frequency (0·52 Hz in both cases) is just a little lower than the natural frequency of the associated system. The simplified method is thus appropriate for the description of the bit motion in stick–slip configuration (the wave

propagation nature of the dynamical system is naturally erased). However for the undamped case for instance, this analogy is less appropriate.

6.2. STATEMENT OF THE PROBLEM

The coupled motion is now considered. The axial modal characteristics are identified as being in torsion (the nature of equation which rules the axial motion is identical to the other direction). As for the torsion motion, a constant axial speed ROP is imposed at the surface and the bit is subjected to a weight which is a function of the bit speeds. The dynamical system is defined by

$$\begin{aligned} m_0\ddot{X} + c_0\dot{X} + k_0(X - \mathrm{ROP}t) &= -\mathrm{WOB}(\dot{X}, \dot{Y}), \\ m_1\ddot{Y} + c_1\dot{Y} + k_1(Y - \Omega t) &= -\varphi(\dot{X}, \dot{Y}). \end{aligned} \tag{33}$$

The same change of variable is adopted:

$$\begin{aligned} x &= X - \mathrm{ROP}t + \frac{\mathrm{WOB}(\mathrm{ROP}, \Omega)}{k_0} + \frac{c_0\mathrm{ROP}}{k_0} \\ y &= Y - \Omega t + \frac{\varphi(\mathrm{ROP}, \Omega)}{k_1} + \frac{c_1\Omega}{k_1}. \end{aligned} \tag{34}$$

According to equation (25) in the previous section,

$$\begin{aligned} m_0\ddot{x} + c_0\dot{x} + k_0x &= \mu\varphi(\mathrm{ROP}, \Omega) - \mu\varphi(\mathrm{ROP} + \dot{x}, \Omega + \dot{y}), \\ m_1\ddot{y} + c_1\dot{y} + k_1y &= \varphi(\mathrm{ROP}, \Omega) - \varphi(\mathrm{ROP} + \dot{x}, \Omega + \dot{y}). \end{aligned} \tag{35}$$

6.3. STABILITY ANALYSIS

Considering the interaction function parameters

$$\gamma = \left.\frac{\partial\varphi(\mathrm{ROP} + \dot{x}, \Omega + \dot{y})}{\partial\dot{x}}\right|_{(0,0)},$$

$$\delta = \left.\frac{\partial\varphi(\mathrm{ROP} + \dot{x}, \Omega + \dot{y})}{\partial\dot{y}}\right|_{(0,0)},$$

the linearization of equation (35) leads to

$$\begin{aligned} m_0\ddot{x} + c_0\dot{x} + k_0x &= \mu(-\gamma\dot{x} - \delta\dot{y}), \\ m_1\ddot{y} + c_1\dot{y} + k_1y &= -\gamma\dot{x} - \delta\dot{y}, \end{aligned} \tag{36}$$

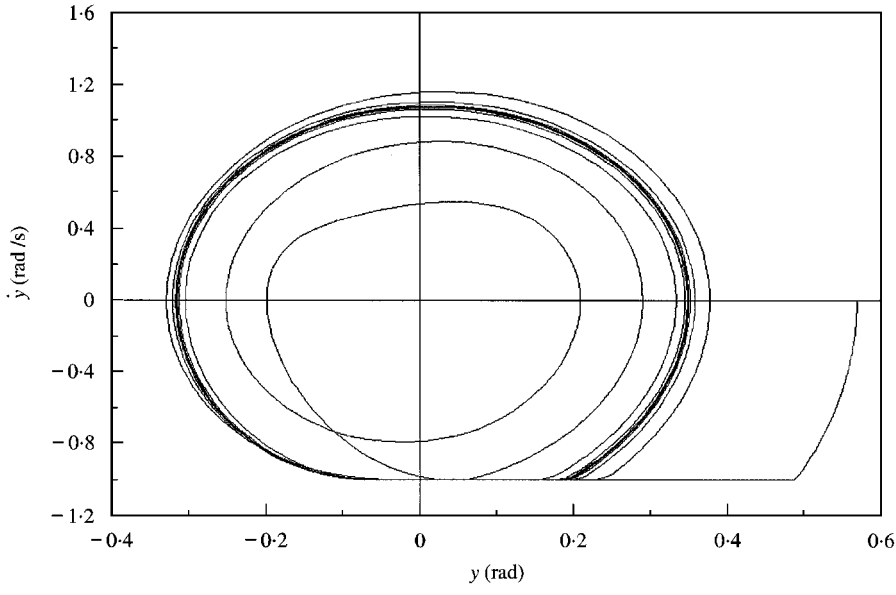

Figure 10. Stick–slip—coupled case.

or, in the same way, to

$$\begin{pmatrix} \ddot{x} \\ \dot{x} \\ \ddot{y} \\ \dot{y} \end{pmatrix} = \begin{pmatrix} -\dfrac{(c_0+\gamma\mu)}{m_0} & -\dfrac{k_0}{m_0} & -\dfrac{\delta\mu}{m_0} & 0 \\ 1 & 0 & 0 & 0 \\ -\dfrac{\gamma}{m_1} & 0 & -\dfrac{(c_1+\delta)}{m_1} & -\dfrac{k_1}{m_1} \\ 0 & 0 & 1 & 0 \end{pmatrix} \begin{pmatrix} \dot{x} \\ x \\ \dot{y} \\ y \end{pmatrix}.$$

The study of the stability of the linearized motion enables the stability of the non-linear system for sufficiently small perturbations to be investigated using the Liapounov theorem. The characteristic polynomial of the undamped system is

$$P(\lambda) = \lambda^4 + a_1\lambda^3 + a_2\lambda^2 + a_3\lambda + a_4,$$

where

$$a_1 = \frac{\gamma\mu}{m_0} + \frac{\delta}{m_1}, \quad a_2 = \frac{k_0}{m_0} + \frac{k_1}{m_1}, \quad a_3 = \frac{k_0}{m_0}\frac{\delta}{m_1} + \frac{k_1\gamma\mu}{m_0 m_1}, \quad a_4 = \frac{k_0 k_1}{m_0 m_1}.$$

The sign of the real part of the polynomial roots is given by Hurwitz criterion. Especially,

$$\begin{vmatrix} a_1 & a_3 & 0 \\ 1 & a_2 & a_4 \\ 0 & a_1 & a_3 \end{vmatrix} = \frac{\gamma\delta\mu}{m_0 m_1}\left(\frac{k_0}{m_0} - \frac{k_1}{m_1}\right)^2.$$

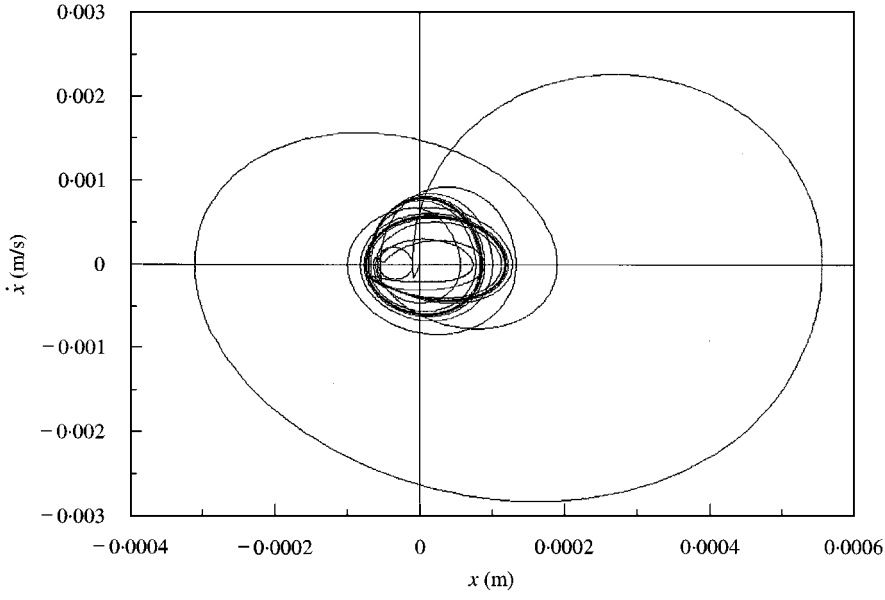

Figure 11. Limit cycle in the axial space.

A necessary stability condition is given by the positivity of this last coefficient. In other words, if γ and δ have opposite signs, the motion is unstable. This is the case of the rock/bit interaction function φ defined previously in equation (24). In particular, equation (36) shows the axial instability. In the more general damped case, the damping is sufficiently small to ensure the validity of the previous conclusion. As will be seen later, this instability is not in contradiction to the quasi-static axial evolution assumption for torsional motion, which is justified by the small oscillations in this axial direction.

6.4. NUMERICAL SIMULATION OF THE COUPLED MOTION

The following parameters, in accordance with the precedent simulation are chosen:

$$m_0 = 37\,278\ \text{kg}, \quad c_0 = 16\,100\ \text{kg/s}, \quad k_0 = 1{\cdot}55 \times 10^6\ \text{kg/s}^2, \quad \text{ROP} = 0{\cdot}01\ \text{m/s},$$

$$m_1 = 147\ \text{kg m}^2, \quad c_1 = 33\ \text{kg m}^2/\text{s} \quad k_1 = 1670\ \text{kg m}^2/\text{s}^2, \quad \Omega = 1\ \text{rad/s},$$

$$\zeta = 1 \times 10^5\ \text{kg m/s}, \quad \mu = 1\ \text{m}^{-1}, \quad \alpha = 0{\cdot}1\ \text{s}.$$

The initial conditions are the same as for the uncoupled system and it is assumed that the axial system is initially in its stationary position.

The trajectory converges to a limit cycle, very similar in the torsion phase plane to the one obtained for the uncoupled motion (the stick–slip frequency is equal to 0·52 Hz again). Only the transitory phase changes (Figure 10). The axial speed evolution has small amplitude, lower in this case than 10% of the mean rate of penetration. Axial motion also describes a limit cycle (Figure 11). This cycle would in fact seem like a point if the scale were to be adapted to the mean value ROP, as is the torsion scale with Ω.

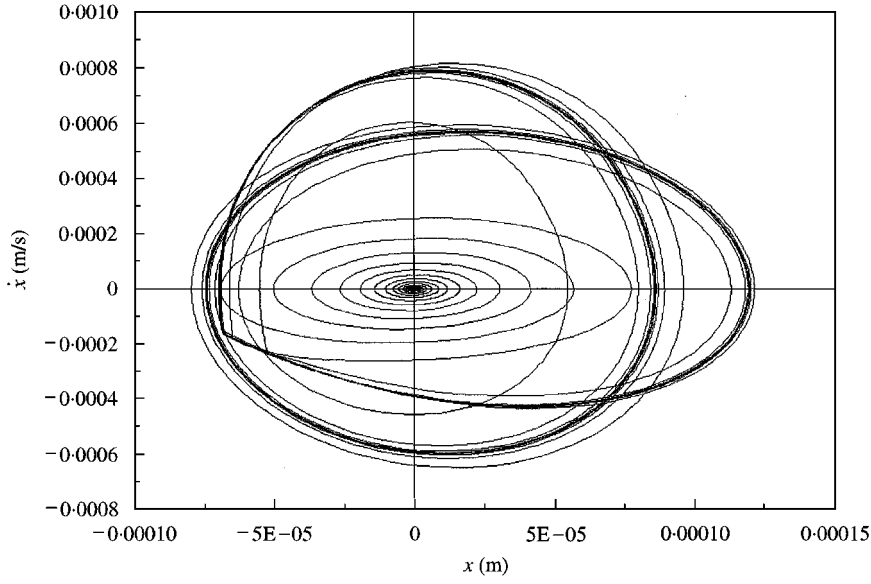

Figure 12. Same limit cycle in the axial space—small perturbation.

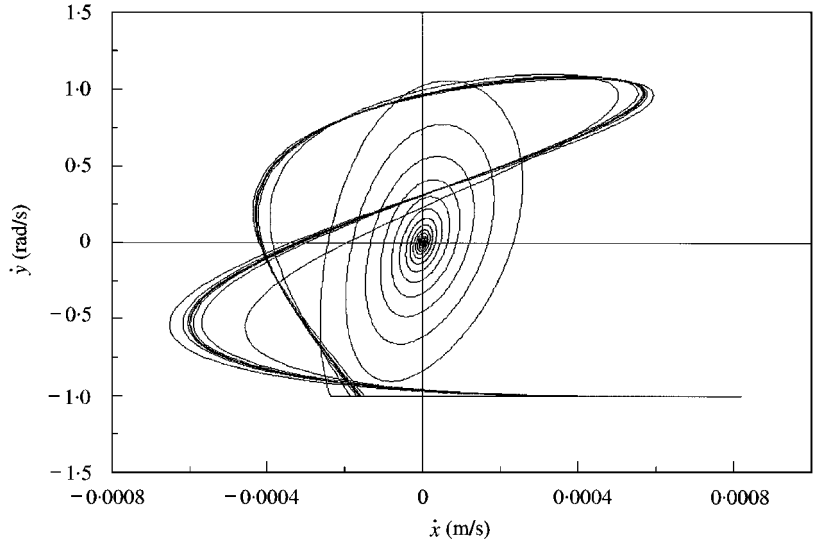

Figure 13. Limit cycle in the speed space.

Simulations with only small perturbation show the particular phenomenon of the limit cycle (Figure 12). The initial conditions are the same as for the stationary solution except for $\dot{y}_0$ which is equal to 0·01 rad/s. The ratio between the fundamental axial and torsion frequency is equal to wave speed ratio when the punctual inertia can be neglected. In the latter case, this ratio is equal to $[2(1 + \nu)]^{1/2}$, equal to 1·6 with the Poisson ratio retained

(the true frequency ratio is 1·9 in the example). The natural axial frequency is greater than the torsion one, and often in the order of twice the natural torsion frequency.

In the simulated case, the fundamental frequency of the axial limit cycle is the same as the stick–slip cycle (torsional plane) but the natural axial frequency is also involved creating two loops in this axial phase plane (related to the ratio between the natural and torsional frequencies). This particular coupling is shown in the phase plane. The limit cycle projected in the speed plane looks like a G clef in music (Figure 13). This plane is important experimentally because these "state" variables are easier to measure than the "position" variables. Such a coupling could be then appreciated during tests.

The trivial solution is asymptotically stable for soft rock ($\varsigma = 1 \times 10^4$ kg m/s for instance). On the contrary, it can be seen numerically that the tendency is accentuated for harder rocks (the stick–slip period growths). Drillers observe such behaviour on rig, when they encounter this dysfunction only in hard formations. The axial boundary conditions have been replaced by a constant weight at the surface, in order to quantify its influence on the evolution of the system. The variation of $\dot{x}$ is of the same order as previously and the stick–slip evolution has not changed. This boundary condition does not play a major role on the global evolution during stick–slip. Finally, simulations indicate that drillstring length tends to increase the coupling, measured by variation of the axial speed with other identical parameters.

7. CONCLUSION

An analytical study has been proposed to characterize the stability of a drilling structure, using the direct method of Liapounov and the linearized method. The stability criterion depends strongly on the form of the rock/bit interaction, linked to the rock destruction process. Simulations illustrate the induced phenomenon. The bit motion can converge towards stick–slip, a typical limit cycle observed during drilling. This phenomenon takes the form of a cone-shaped limit surface concerning the beam, which can generate detrimental fatigue on drillpipes. The stick–slip phenomenon, often noticed in drilling mechanics, has been modelled using the knowledge of rock mechanics. Drilling stick–slip behaves for PDC bits with very small variation of axial speed and most often justifies the use of an uncoupled model in torsion [17]. The simultaneous use of non-linear dynamics and rock mechanics must be completed to generalize these results to lateral evolution.

ACKNOWLEDGMENTS

The author is indebted to D. Girardot, P. Rouchon, J. Salençon and H. Sellami for their valuable help.

REFERENCES

1. M. P. Dufeyte and H. Henneuse 1991 *S.P.E* 21945. Detection and monitoring of the stick–slip motion: field experiments.
2. A. P. Christoforou and A. S. Yigit 1997 *Journal of Sound and Vibration* **206**. Dynamic modelling of rotating drillstrings with borehole interactions.
3. V. A. Palmov, E. Brommundt and A. K. Belyaev 1995 *Dynamics and Stability of Systems* **10**. Stability analysis of drillstring rotation.
4. A. K. Belyaev and E. Brommundt 1994 *Zeitschrift für Angewandte Mathematik und Mechanik* **74**. Influence of the motor and bit characteristics on the stability of drillstring rotation.

5. V. A. DUNAYEVSKY and F. ABBASSIAN 1995 *S.P.E.* 30478. Application of stability approach to bit dynamics.
6. S. P. TIMOSHENKO 1955 *Vibrations Problems Engineering*. Princeton, NJ: D. Van Nostrand Company.
7. A. A. MOVCHAN 1960 *P.M.M.* **24**. Stability of processes with respect to two metrics.
8. R. J. KNOPS and E. W. WILKES 1966 *International Journal of Engineering Science* **4**. On Movchan's theorems for stability of continuous systems.
9. P. HAGEDORN 1978 *Non Linear Oscillations*. Oxford: Oxford Science Publications.
10. A. HARAUX 1991 *Systèmes dynamiques dissipatifs et applications*. Paris: Masson.
11. N. CHALLAMEL 1998 *Revue Française de Géotechnique* **84**. Calcul à la rupture appliqué à la coupe de géomatériaux.
12. N. CHALLAMEL and H. SELLAMI 1998 *S.P.E* 47340, *Eurock*'98, *Trondheim*, *Norway*. Application of yield design for understanding rock cutting mechanism.
13. N. CHALLAMEL 1999 9*th International Congress On Rock Mechanics*, *Paris*, *France*. Rôle de la microstructure dans le processus de coupe des roches.
14. E. DETOURNAY and P. DEFOURNY 1992 *International Journal of Rock Mechanics*, *Mining Science and Geomechanical Abstracts* **29**, 13–23. A phenomenological model for the drilling action of drags bits.
15. A. LESEULTRE and E. LAMINE 1998 *S.P.E.* 39341. An instrumented bit: a necessary step to the intelligent BHA.
16. D. R. PAVONE and J. P. DESPLANS 1994 *S.P.E.* 28234. Application of high sampling rate downhole measurements for analysis and cure of stick–slip in drilling.
17. N. CHALLAMEL, H. SELLAMI and E. LAMINE 1999 *Congrès Français de Mécanique*, *Toulouse*, *France*. Bifurcation en dynamique du forage.
18. T. V. AARRESTAD and A. KYLLINGSTAD 1986 *S.P.E.* 15563. An experimental and theoretical study of coupled boundary conditions for vibrations in drillstring.
19. C. J. LANGEVELD 1992 *S.P.E.* 23867. PDC bit dynamics.
20. J. P. DEN HARTOG 1934 *Mechanical Vibrations*. New York: Dover Publications Inc.
21. J. D. JANSEN and L. VAN DEN STEEN 1995 *Journal of Sound and Vibration* **179**. Active damping of self-excited torsional vibrations in oil well drillstrings.